The effect of bioartificial constructs that mimic myocardial structure and biomechanical properties on stem cell commitment towards cardiac lineage.

(Article begins on next page)

11 March 2025

UNIVERSITÀ DEGLI STUDI DI TORINO

The effect of bioartificial constructs that mimic myocardial structure and biomechanical properties on stem cell commitment towards cardiac lineage

Cristallini C.[a]*, Cibrario Rocchietti E.[b]**, Accomasso L.[b], Folino A.[b], Gallina C.[b], Muratori L.[b], Pagliaro P.[b], Rastaldo R.[b], Raimondo S.[b], Saviozzi S.[b], Sprio A.E.[b], Gagliardi M.[c], Barbani N.[c], Giachino C.[b]

[a] Institute for Composite and Biomedical Materials, C.N.R., o.u. Pisa, Pisa, 56122, Italy

[b] Department of Clinical and Biological Sciences, University of Turin, Orbassano (Turin), 10043, Italy

[c] Department of Civil and Industrial Engineering, University of Pisa, Pisa, 56122, Italy

Corresponding authors:

* Institute for Composite and Biomedical Materials, C.N.R., o.u. Pisa, Largo Lucio Lazzarino, 56122 Pisa, Italy. Telephone: (+39)0502217802. Fax : (+39)0502217866. e-mail: caterina.cristallini@diccism.unipi.it.

** Department of Clinical and Biological Sciences, University of Turin, Regione Gonzole 10, 10043 Orbassano (TO), Italy. Telephone: (+39)0116705425. Fax: (+39)0119038639. e-mail: elisa.cibrariorocchietti@unito.it.

RUNNING TITLE

The cardioinductivity of PHBHV/gelatin constructs on stem cells

ABSTRACT

Despite the enormous progress in the treatment of coronary artery diseases, they remain the most common cause of heart failure in the Western countries. New translational therapeutic approaches explore cardiomyogenic differentiation of various types of stem cells in combination with tissue-engineered scaffolds. In this study we fabricated PHBHV/gelatin constructs mimicking myocardial structural properties. Chemical structure and molecular interaction between material components induced specific properties to the substrate in terms of hydrophilicity degree, porosity and mechanical characteristics. Viability and proliferation assays demonstrated that these constructs allow adhesion and growth of mesenchymal stem cells (MSCs) and cardiac resident non myocytic cells (NMCs). Immunofluorescence analysis demonstrated that stem cells cultured on these constructs adopt a distribution mimicking the three-dimensional cell alignment of myocardium. qPCR and immunofluorescence analyses showed the ability of this construct to direct initial MSC and NMC lineage specification towards cardiomyogenesis: both MSCs and NMCs showed the expression of the cardiac transcription factor GATA-4, fundamental for early cardiac commitment. Moreover NMCs also acquired the expression of the cardiac transcription factors Nkx2.5 and TBX5 and produced sarcomeric proteins. This work may represent a new approach to induce both resident and non-resident stem cells to cardiac commitment in a 3-D structure, without using additional stimuli.

Abbreviations: 3-D, Three-dimensional; ECM, Extracellular Matrix; MSCs, Mesenchymal Stem Cells; NMCs, Non Myocytic Cells; PHBHV, Poly(3-hydroxybutyric acid-co-3-hydroxyvaleric acid).

1. INTRODUCTION

Myocardial infarction causes heart muscle loss and decrease of function. Although surgical and pharmacological therapies have improved the survival of patients, these therapies cannot effectively compensate for the loss of cardiomyocites [1]. Recently, stem cell therapy has emerged as a promising approach for both heart regeneration and function restoration [2, 3].

Various types of stem cells have cardiac commitment potential, including mesenchymal stem cells (MSCs) [4-6] and cardiac resident progenitor cells [7]. Some of the initial efforts at promoting cardiomyogenesis using MSCs involved the use of the demethylating agent 5-azacytidine [8], which, however, induces apoptosis *in vivo* [9]. Thereafter, a variety of different approaches have been attempted, including electrical stimulation, chemical induction, use of biological agents and cell co-culturing. However, evidence of MSC differentiation to a cardiomyogenic phenotype *in vivo* has been controversial [10], leading to the concept that functional benefits of MSCs may be largely due to paracrine mechanisms [11, 12]. New hope for cardiac tissue regeneration has been raised by the discovery of resident cardiac stem cells in the adult murine heart [7]. Several recent reports demonstrated that clonally expanded human cardiac progenitor cells [13-15] can generate new viable myocardium and support ventricular function when injected into infarcted hearts [16]. However the delivery of stem cells and the timing of their implantation are particularly problematic, leading to the loss of up to 90% of transplanted cells soon after delivery due to hypoxia, myocardial inflammation, or the physical stresses associated with the implantation procedure [17, 18]. Since the cell niche provides crucial support [19-21], tissue-engineered scaffolds, resembling the characteristics of the native tissue, may be a feasible therapeutic approach. In fact biomaterials have been increasingly used in targeting heart repair [22, 23], as they can provide a proper platform for stem cell survival, proliferation and differentiation, as well as a guide for three-dimensional (3-D) tissue

reconstruction [24]. Proper myocardium regeneration and function may be largely dependent on the properties of the scaffolds. For instance, biomimetic scaffolds mimicking features of the myocardial extracellular matrix (ECM) may facilitate tissue development, as they provide a native-like template that allows cells to organize into the tissue specific structure [25, 26]. Yet, the effectiveness of stem cell therapy depends on proper cell differentiation, thus the ideal tissue constructs should stimulate correct stem cell commitment towards cardiac lineage.

Over the past years, polyhydoxyalkanoates (PHAs) were used as biomaterials for applications in medical devices and tissue engineering scaffolds [27]. Poly 3-hydroxybutyrate (PHB) was also investigated for cardiovascular patches [28]. 3-D scaffolds consisting of pure gelatin have already been applied for the regeneration of cardiac tissue both *in vitro* and *in vivo*. In particular, *in vitro* tests have shown spontaneous rhythmic contractility and cell migration of cells seeded on these structures [29]. Yet *in vivo* tests showed a dissolution process of gelatin patches, which starts at four weeks and is over at twelve with inflammatory response [30]. However there is no information in literature about the use of 3-hydroxybutyrate and 3-hydroxyvalerate (PHBHV) as pure polymer or in combination with biological polymers for cardiac reconstruction.

We hypothesized that a construct for cardiac regeneration with optimal characteristics could be obtained by combining gelatin, providing good biocompatibility and adequate degradation kinetics with PHBHV having easy processability and a minimal inflammatory response. Moreover, the non-crosslinked gelatin introduced in the bioartificial system can favor water adsorption into the scaffold enhancing hydrolytic degradation of synthetic component. Therefore, we investigated the role of chemical composition and surface properties of the substrates in controlling stem cell response. Chemical structure and molecular interaction between material components give different properties to the substrate including hydrophilicity/hydrophobicity, roughness, porosity, chemical

compatibility, mechanical characteristics and degradation kinetics associated to the material in analogy to those of the native tissue [31, 32]. One important aspect is to select material microstructure geometry depending on the specific cell type of which is to promote growth. Recently, cell adhesion of cardiomyocytes was increased by honeycomb structures with pores slightly higher than cells [33]. Increased elongation efficiency of human MSCs (hMSCs) was observed on polycaprolactone (PCL) substrates having anisotropic geometry obtained by uniaxial stretch [34]. Aligned fibrous scaffolds of biodegradable polyurethane, obtained by electrospinning, improved the differentiation of murine embryonic stem cell-derived cardiomyocytes in co-culture with fibroblasts [35]. Hence, in this study we investigated whether PHBHV/gelatin tissue constructs, which have specific physico-chemical properties and a micro-topography that mimics structural and mechanical properties of the myocardium, would induce MSCs and cardiac resident cells (non myocitic cells, NMCs) to differentiate into a cardiac lineage without the need for additional stimuli.

2. MATERIALS AND METHODS

2.1 Preparation and physico-chemical/mechanical characterization of PHBHV/gelatin scaffolds

2.1.1 Reagents

Poly(3-hydroxybutyric acid-co-3-hydroxyvaleric acid) (PHBHV, Sigma-Aldrich, USA, , PHV content 12% mol) and gelatin from porcine skin [gelatin A (GelA), Sigma-Aldrich] were used without further purification for scaffold preparation. As solvent, dichloromethane (DCM, Carlo Erba Reagenti, Italy, ACS purity degree) and milliQ water were used for the preparation of PHBHV and GelA solutions respectively.

2.1.2 Preparation of bioartificial blends

Bioartificial blends were obtained starting from different solutions of PHBHV/DCM and a GelA/water solution with concentration 10% w/v obtained at 50°C. Polymer solution was maintained under high stirring at room temperature and the gelatin solution was added dropwise to avoid the segregation of the protein in DCM. Four different PHBHV/gelatin blends were prepared with following composition (w/w): 95/05, 90/10, 85/15 and 80/20 [36].

2.1.3 Preparation of ECM-like porous bioartificial membranes

Using prepared blends, microstructured scaffolds were obtained by soft lithography. The geometry of the ECM-like scaffold and the procedure to obtain the geometry, based on the morphological analysis of a decellularized suine cardiac tissue, were already described in a previous work [34]. A productive drawings obtained by CAD systems has been realized in accordance with the predefined geometry. CAD model was applied to soft lithography technique to obtain a silica master and the corresponding soft moulds were prepared by polymerization of a vinyl-terminated polydimethylsiloxane (PDMS) oligomer (Sylgard® 184 Silicone Elastomer Kit, Dow Corning Corporation, USA) in an under-vacuum oven at 40°C for 24 h. At the end of the polymerization, the soft mould was cut around the silica master and carefully removed. A predefined volume of bioartificial blend obtained as previously described was deposited by using a Gilson syringe on the PDMS mould then lyophilized for 18 h to obtain a controlled solvent casting and homogeneous microstructured materials. Bioartificial blends were laid on glass flat supports and the same procedure previously described was followed to obtain non-microstructured materials as control. Thickness of obtained biomatrices varied on the basis of the chemical composition of the bioartificial blend from 70 μm to 300 μm.

2.1.4 Scaffold characterization

Morphological analysis was carried out onto Au sputtered samples by scanning electron microscopy (SEM, Jeol JSM 5600, Japan). Chemical analysis was carried out by FT-IR Chemical Imaging (Perkin Elmer Spotlight 300, USA) and high-performance liquid chromatography (HPLC, Perkin Elmer Series 200, USA); for FT-IR analysis, a) attenuated total reflectance (ATR) sampling technique on small fragments of scaffolds was performed, the use of the Chemical Imaging allowed evaluating the distribution of components in the manufacts, obtaining chemical and correlation maps to visualize their distribution, b) near infrared spectroscopy was used to evaluate anisotropic hydrophilicity (FT-NIR Spectrum 400, Perkin Elmer, USA). Spectral images were acquired in transmission and µATR mode (spectral resolution was 4 cm^{-1}, spatial resolution was 100x100 µm) using the infrared imaging system Spotlight 300 (Perkin Elmer). Spectra were collected by touching the ATR objective on the sample and collecting the spectrum generated from the surface layer of the sample. The Spotlight software used for acquisition was also used to pre-process the spectra. Near infrared spectra were measured in the region 7800-4000 cm^{-1} in reflection mode at spatial resolution of 6.25 µm; Dynamic mechanical analysis was performed by DMA (DMA8000, Perkin Elmer, USA) to evaluate the viscoelastic behavior of the materials at different temperatures, samples (length 1 cm, width 0.5 cm, thickness dependent on the composition) underwent a strain scan analysis, imposing a cyclic deformation of 5% in respect to sample length, tests were carried out in dry and wet conditions, at room temperature and at 37°C. In addition, in order to evaluate the mechanical anisotropy of obtained scaffolds, tests were carried out applying the strain in two directions, parallel and perpendicular to the grating direction. Mechanical parameters of the microstructured materials were evaluated taking the cross section geometry into account. In particular, the actual section of microfabricated specimens was evaluated as:

$$A_{act} = l \cdot s - n_c \cdot l_2 \cdot s \qquad \text{(Eq. 1)}$$

Where A_{act} is the actual cross section, l is the width of the matrix, s is the thickness, nc is the number of unit cells that were repeated along the width of the sample, l_2 is the sum of the widths of cell voids along the sample width. The value of A_{act} was divided by the sample width to obtain an actual width l_{act}. With this parameter the geometry constant K was evaluated as:

$$K = \frac{l_{act} \cdot s}{L \cdot 1000} \qquad \text{(Eq. 2)}$$

Where L is the length of the sample. K is the requested parameter that the software used to convert measured stiffness values into modulus.

Degradation analysis was carried out *in vitro* on selected scaffolds, tests were conducted up to six months in three different media: bidistilled water, Phosphate Buffered Saline (PBS), Dulbecco's Modified Eagle Medium (DMEM, Life Technologies, USA). Degradation samples underwent SEM, FTIR and gel permeation chromatography (GPC, Perkin Elmer, USA) analyses; SEM analysis allowed evaluating how scaffold morphology changed after degradation; FTIR evaluated the variation of chemical compositions of samples; the molecular weight lowering and the variation of polydispersity index of PHBHV matrix were quantified by GPC, obtaining degradation kinetic profiles. For GPC analysis, a Perkin Elmer pump, equipped by a ResiPore (Agilent Technologies, USA) column, UV and RI detectors, were used; internal mobile phase was composed of THF (1 ml/min), analysis was carried out at room temperature; results were obtained basing on a calibration curve obtained with polystyrene narrow standards. Finally, pH of degradation medium was monitored during time using pH-meter.

DSC analysis was carried out to evaluate temperatures and enthalpies related to thermal events, in the range of 30-300°C using a differential scanning calorimetry (DSC 7, Perkin

Elmer, USA); sample were placed in aluminium pans at the rate of 10°C/min under nitrogen flux.

2.2 Seeding and culture of cells on PHBHV/gelatin scaffolds

Isolation and characterization of cells were performed as described in Supplementary data section. Depending on the experiments, between 5×10^3 and 20×10^3 cells were resuspended in 50 µl of complete α-MEM (α-Minimum Essential Medium) or DMEM medium (Life Technologies) supplemented with 10% fetal bovine serum (FBS, Euroclone, Italy) and seeded in drops on the surface of the PHBHV/gelatin scaffolds placed in 24-well plates. After 3 hr necessary for cell adhesion, 500 µl of complete medium were added to cover the scaffolds and then samples were kept in an atmosphere of 5% CO_2, 95% air at 37°C in a humidified incubator. Cells seeded on the scaffolds were maintained in culture for up to two weeks and medium was replaced every 3 days. For 2-D control condition, 4×10^3 cells/cm^2 were seeded and harvested at 80% confluence.

2.3 Adhesion and proliferation assays

Cell adhesion was evaluated after 24 h of culture using the metabolic assay CellTiter-Blue (Promega, USA), which assesses the redox activity of living cells by conversion of resazurin dye into the fluorescent product resorufin; thus, fluorescence measured in the medium is proportional to the number of living cells. Cells were seeded on PHBHV/gelatin scaffolds and simultaneously on a 24 well plate to create a calibration curve (0, 1250, 2500, 5000, 10000, 20000 cells/well). After 24 h of culture resazurin was added in the medium of each well at a 1:10 ratio and incubated for 3-5 h. Then the supernatant from each well was collected in a 96 well plate and fluorescence emission was read at 590 nm with a multi-plate reader (Infinite F200, Tecan, Switzerland). To calculate the percentage of cell adhered to the constructs, values of the calibration curve were used to compare the

fluorescence measured from cellularized scaffolds. For proliferation analysis , CellTiter-Blue assay was repeated on the same cellularized samples at 4, 8, 12, 15 days after seeding; in this set of experiments fluorescence emission from each sample was normalized on its initial value at 24 h. After each test cellularized scaffolds were washed twice with 1X PBS and then fresh medium was added to continue the culture.

2.4 Cell morphology and alignment analysis

For immunofluorescence analysis of cell morphology, cytoskeletal organization and colonization of scaffolds, cellularized scaffolds were processed at room temperature. Briefly, samples were washed twice with PBS and subsequently fixed with 4% paraformaldheyde (PAF, Sigma-Aldrich) for 30 min, prior to permeabilizing with 0.1% Triton X-100 for 15 min and blocking with 6% bovine serum albumin (BSA, Sigma-Aldrich) and 2.5% normal goat serum (NGS, Sigma-Aldrich) for 1 h. Actin filaments and nuclei were then stained respectively with red phalloidin 1:200 (Sigma-Aldrich) for 30 min and 4'-6-Diamidino-2-phenylindole (DAPI) 1:100 (Sigma-Aldrich) for 20 min. After mounting on glass slides with Mowiol aqueous solution (Calbiochem, USA), cellularized scaffolds were analyzed by confocal microscopy (TCS-SPE, Leica Microsystem, Germany).

Cell alignment and elongation were evaluated with Calcein-AM (Sigma-Aldrich), a cell-permeant molecule, which is cleaved by intracellular esterases to produce a green fluorescent dye that is retained in the cytosol of living cells. Cellularized scaffolds were stained with 2 µmol/L Calcein-AM for 30 min at 37°C and then analyzed by confocal microscopy (Carl Zeiss Laser Scanning System LSM 510, Germany). The staining was repeated on the same scaffolds at 1, 4, 8, 12 and 15 days of culture. 3-D reconstructions were obtained with Imaris 7.6.1 (Bitplane Scientific Solution, Switzerland). hMSC and NMC mean cell length was analyzed at 1, 3, 12 days of culture using ImageJ® ROI measure tool (Rasband, W.S., ImageJ, U.S. National Institutes of Health, USA,

http://rsb.info.nih.gov/ij/, 1997-2012). 2-D control cultures refer to the mean cell length evaluated on confocal images of both cell types cultured for 3 days on 24-well plates in order to reach the maximum elongation.

For transmission electron microscopy, hMSCs cultured on the scaffolds for 3 days were fixed in 1% PAF (Merck, Germany), 1.25% gluteraldehyde (Fluka, USA) and 0.5% saccharose in 100 mmol/L Sörensen phosphate buffer (pH 7.2) for 2 h. Samples were then washed in 1.5% saccharose in 100 mmol/L Sörensen phosphate buffer (pH 7.2) for 6–12 h, post-fixed in 2% osmium tetroxide, dehydrated and embedded in Glauert's embedding mixture, which consists of equal parts of Araldite M and Araldite Härter, HY 964 (Merck), supplemented with the plasticizer dibutyl phthalate at 0.5%. The accelerator DY 064 (Merck) was added at 2%. Thin sections (70 nm) were cut using a Leica Ultracut UCT, stained with uranyl acetate and lead citrate and examined in a JEM-1010 transmission electron microscope (JEOL, Japan) equipped with a Mega-View-III digital camera and a Soft-Imaging-System (SIS, Germany) for computerized acquisition of images.

2.5 RNA extraction, cDNA Synthesis, qPCR and reverse transcriptase PCR (RT-PCR)
Cellularized scaffolds were dissolved in TRIzol reagent (Life Technologies) and total RNA (totRNA) was extracted according to the manufacter's instructions. Genomic DNA contaminations were removed by DnaseI treatment (Ambion, USA) and RNA was then quantified. One microgram of totRNA was finally retrotranscribed with random hexamer primers and Multiscribe Reverse Transcriptase contained in High Capacity Reverse Transcription Kit (Applied Biosystems, USA) in accordance with manufacter's suggestions. Expression levels of all target genes and one reference gene (Polr2) were evaluated with SYBER green technology on an ABI PRISM 7500 Fast Real-Time PCR system (Applied Biosystems) using 25 ng of cDNA template and 150µM of each primer (listed in Supplementary Table 3). Melting curve analysis was performed for all amplicons. For each

target gene, fold change in expression levels between cellularized scaffolds and 2-D control culture was evaluated with the $2^{-\Delta\Delta Ct}$ method using Pol2r as reference gene and matched 2-D control culture as calibrators. RT-PCR of Mef2c was performed as described in Supplementary data.

2.6 Immunofluorescence characterization of cells cultured on microstructured PHBHV/gelatin scaffolds

For immunofluorescence analysis of cardiomyogenic markers after 15 days of culture, both 2-D control and cells seeded on the scaffolds were detached using 0.25% trypsin-1mmol/L EDTA (Life Technologies) and cytospinned at 250 rpm for 6 min. Cells were then fixed with 4% PAF for 15 min, permeabilized with 0,1% Triton for 5 min and blocked in 10% FBS for 1 h. Primary antibodies (see Supplementary Table 2) were diluted in 1X PBS supplemented with 1% FBS and then incubated O/N at 4°C. After two washes in 1X PBS-0,1% Tween, cells were incubated with secondary antibodies (see Supplementary Table 2), diluted 1:1000 in 1X PBS, for 1 h at RT and then cell nuclei were stained with DAPI 1:100 for 20 min. Coverslips were mounted with Mowiol aqueous solution and analyzed by confocal microscopy (TCS-SPE, Leica Microsystems).

2.7 Statistical Analysis

All results are expressed as mean ± standard error of the mean (S.E.M.). Statistically significant differences between any two groups were determined using the paired Student t test and differences with $p \leq 0.05$ were regarded as statistically significant.

3. RESULTS

3.1 PHBHV/gelatin Myocardial scaffold preparation and characterization

3.1.1 Morphological analysis

SEM images of microfabricated material surfaces showed a macroporosity and a meso-microporosity independently from the material composition (Fig.1 A). For each composition, it can be seen the presence of rectangular recesses following the soft lithography model geometry and micro-mesopores distributed diffusely at the level of the entire structure due to chemical composition and solvent casting procedure (Fig.1 A). The macrocavities, considered as polymeric guides to induce alignment of cardiomyocytes have longitudinal and trasversal dimension of 480 μm and 25 μm and a depth of 40 μm, and are separated among them by an array of longitudinal regular ridges of 60 μm and 25 μm and cross ridges of 30 μm. SEM images of non-microstructured matrices show an isotropic distribution of micropores having diameter of 5-20 μm (Fig.1 A). Pore dimension resulted dependent on both weight composition of bioartificial material and concentration of polymeric solution: a higher content of gelatin as well as a higher concentration of PHBHV solution determined an increase of pore dimensions.

3.1.2 FT-IR Chemical Imaging
Chemical analysis allowed to evaluate a series of surface parameters: hydrophilicity, chemical homogeneity, molecular interactions, distribution and conformation of protein component.

Hydrophilicity
The absorption band at 3700-3000 cm^{-1} contains a number of vibration modes related to hydroxyl groups including those of adsorbed water and to NH stretching. For this reason this band can be considered an index of material hydrophilicity degree. From map analysis carried out on various PHBHV/gelatin materials (95/05, 90/10, 80/20), the ratio between

the band at 3700-3000 cm^{-1}, and the band at 3000-2840 cm^{-1} related to C-Hx stretching was calculated. The same analysis was carried out on samples of porcine healthy myocardium tissue, previously dried and treated under the same conditions of the polymeric materials and the results were compared. Since maps were acquired in µATR mode, the obtained values can be representative of surface hydrophilicity of prepared materials. All the maps were characterized by a minimum value registered in the zone where protein was more uniformly blended with synthetic component (C-O-H/C-Hx ratio, 0.45-1.0) and by a maximum value measured in the zones with a higher density of protein (C-O-H/C-Hx ratio, 1.5-4.0). It is important to underline that this variability of band ratio is typical also of the natural tissue; moreover the values measured for the blends resulted comparable with those obtained for native myocardium samples (C-O-H/C-Hx ratio, 2.0-3.4).

In addition the near infrared spectroscopy was used to evaluate the surface hydrophilicity of a selected microstructured sample (95/05 PHBHV/gelatin) showing eventual distinct changes along the features of micropatterning. In particular hydrophilicity is strictly associated to the presence of hydrophilic groups of polymeric chains but also to the porosity characteristics of material. For this reason, two distinct bands were selected at 6000-5300 cm^{-1} associated with the first overtone of CH stretching vibrations and at 5462-4943 cm^{-1} corresponding to first OH overtone of water adsorbed into the samples [37]. The map was acquired in function of the ratio of band (νOH/νCH) (Fig 2). The visualization of the map correlated with the band ratio shows the presence of darker zones at level of the recesses of microstructure where the band ratio was 0.4-0.6. In correspondence of the ridges of microstructure the values of the ratio measured resulted lower in the range 0.1-0.3. These results indicated that there is a greater ability to bind water inside the cells with respect to the reliefs. Then, PHBHV/gelatin showed anisotropic surface hydrophilicity, with higher amount of hydrophilic groups along the floor of the cell configuration.

Chemical homogeneity, molecular interactions, conformation of protein component

FT-IR spectra were obtained by difference maps of PHBHV/gelatin at various compositions, each spectrum showed the characteristic bands of both polymers including the bands at 1800-1650 cm^{-1} (C=O stretching), at 1663 cm^{-1} (amide I, CO stretching) at 1550 cm^{-1} (amide II, NH bending and CN stretching). The correlation maps respect to the bands of the protein typical region (amide I and II), obtained using instrument software, showed an heterogeneous distribution of gelatin on matrix surface with domains at variable protein aggregation depending on matrix composition (Fig 3). Domains with a more homogenous distribution of protein component were observed by decreasing gelatin content: an important result refers to evidence of a shift of amide I band (1634 cm^{-1}) towards higher frequencies (1661 cm^{-1}), as shown in figure 3, indicating the existence of molecular interactions between two components.

In the areas in which the gelatin resulted more homogeneously distributed, the second derivative spectra acquired from the maps of materials at different compositions were analyzed (Fig 4). Deconvolution of amide I band, relevant for identification of polypeptide conformation, showed the presence of peaks, that can be attributed to β-turn conformation (1663 cm^{-1}), α helix (1648 cm^{-1}) and unordered forms (1630 cm^{-1}) [38]. The same analysis carried out on a sample of pure gelatin showed a strong variability of bands relative to amide I deconvolution: peaks among 1670-1665 cm^{-1} and among 1635-1620 cm^{-1} corresponding to β-turn conformation and to displacements of the unordered conformation, shifted towards lower frequencies as a consequence of the high number of hydrogen bond interactions that the denatured protein can establish.

The results seemed to show a partial reorganization of gelatin chains due to the presence of a prevalence of β-sheet structures in addition to α helices, triple helices (1638 cm^{-1}) and unordered forms [39, 40].

3.1.3 Thermal analysis

The thermograms of pure PHBHV material showed two close endothermic events, both due to the melting of crystalline zones, the first event at 152°C and the second one, although of minor intensity, at 140°C. This result highlights the presence of a polymorph structure characterized by two crystalline domains with different structures. The thermograms related to the blends showed the presence of the same endothermic events observed in the case of pure PHBHV. No variation was detected in terms both of melting temperature values and in terms of total enthalpy (40 J/g), indicating that the presence of gelatin did not appreciably altered the crystallinity of bioartificial matrix.

3.1.4 Mechanical analysis

The results of stress-strain tests evaluated for non-microstructured PHBHV/gelatin at various ratio showed deformation values in the range of 25-30% and elastic modulus of 4-5 MPa. The curves of strain scan tests exhibited a decrease of storage modulus E' and loss modulus E'' with the increasing of deformation percentage. Multi- frequency tests, carried out both under dry and wet conditions, showed no substantial difference of E' and E'' by varying the frequency. Storage modulus of 4÷6 MPa and 2÷5 for dry and wet conditions, respectively, were registered.

Particular attention was paid on mechanical characterization of microstructured 95/05 PHBHV/gelatin system compared to the non-microfabricated material with the same composition. Samples were analysed by means strain scan tests both in dry and wet conditions to evaluate the trend of sample rigidity as function with tensile strain. Since microstructured samples have a anisotropic geometry, tensile tests were carried out under dry and wet conditions at 37°C in both transverse and parallel directions to the micropatterning. For not microfabricated biomatrices, tensile tests at 37°C were carried out

in one direction because there is no orientation in the sample. Tests were performed in triplicate.

By the comparison between results obtained for microstructured and non-microstructured materials, a substantial difference in the modulus value along two different directions for microfabricated was registered (Fig.1 B, C). This result may be attributed to the anisotropy of microfabricated structure, composed of elements with different lengths and cross-sections and thus different stiffness. A preferential alignment of polymeric chains is taken within the structure along the edges of the cavities. On the contrary, the membrane having an isotropic structure without a preferential alignment showed a storage modulus in longitudinal direction lower than that measured for microstructured material (Fig. 1 C). From the comparison of the microfabricated system 95/05 PHBHV/gelatin, subjected to dry and wet tests, a decrease of E' was detected. E' values obtained under water immersion conditions resulted lower than those measured under dry conditions and thus more in agreement with the application (Fig. 1 C).

3.1.5 Degradation analysis

A complete degradation analysis was carried out *in vitro* on selected scaffolds, the tests were conducted also in culture medium (DMEM, to better simulate physiological condition) and for prolonged times up to six months in three different media (bidistilled water, PBS, DMEM). At fixed and close times, both incubation medium for pH analysis and degraded samples by means loss mass, morphology variation, GPC analysis and thermal behavior were analyzed.

pH tests

In general, pH measurements of the incubation media up to six months for the three different media, showed a dense distribution of values in the physiological range the whole

period of time. This behavior if, on the one hand, reflects the stability of the material to prolonged times, on the other indicates that the low percentage of degradation products does not alter the pH conditions.

In all three cases, it can be observed how the pH value is maintained in a range between 6 and 8 (Fig 5 C).

Morphological tests

SEM images of the section and surface for the samples analyzed at different degradation times (7, 15, 90, 135 and 180 days) were collected. In fig. 5 A SEM images of surface of microstructured 95/05 PHBHV/gelatin samples after degradation in three different incubation media after 15 and 180 days were reported.

Morphological analysis showed that the micropatterning remained almost unaltered indipendently from degradation conditions (Fig. 5 A). This could be due to the slow degradation kinetic of the bioartificial material, as confirmed also by gravimetric tests indicating a modest variation in weight over time.

Gravimetric and GPC tests

The kinetic of weight loss for pure PHBHV material is very slow and reaches weight change values of about 4% respect to initial weight, while bioartificial materials show a kinetic of weight loss more rapid than pure material (up to 12% after 42 days). This result is mainly attributed to a fast release of gelatin from biomatrix. Concerning GPC results, curves of weight average molecular weight (Mw) versus time of bioartificial systems present all a more rapid decrease respect to pure PHBHV and an acceleration of decline with the increasing of gelatin content (Fig 5 B). In particular, after about 40 days of incubation, a decrease of Mw from 30 to 59% was measured moving from PHBHV/gelatin composition 95/05 to 80/20. Measurements of number average molecular weight (Mn)

exhibit a slow and gradual variation versus time independently from composition ratio, in addition the trend of polydispersity index (PDI) with time is indicative of an homogenous degradation of polymeric biomatrix (supplementary data).

Thermal analysis

No significant variation in the melting temperature as a function of degradation time was observed, on the contrary it is evident a remarkable increase of melting enthalpy (ΔH_{tot} from 30.8 to 41.2 J/g after 42 days) of samples subjected to degradation tests. This result is in agreement with the fact that degradation involves mainly amorphous zones of polymeric material due to the higher flexibility of chains respect to crystalline domains. An increase of specific enthalpy is a consequence of an increase of crystalline fraction inside the sample.

3.2 Stem cell growth and alignment

MSCs and NMCs were cultured on non-microstructured and microstructured PHBVH/gelatin scaffolds and cell morphology and viability were monitored on both constructs up to at least 15 days of culture, using Calcein-AM staining. The biocompatibility experiments were performed with all four bioartificial compositions obtaining comparable results for all materials, for this reason the results will be documented by representative images of different specific blends. Notably, only on microstructured scaffolds cells adopted a stretched morphology and aligned in parallel to each other in a similar way to cell organization in native myocardium (Fig 6, B and C), whereas on non-microstructured scaffolds cells kept a round shape without elongation and this morphology was maintained over time (Fig 6 A). 3-D reconstructions documented the ability of living cells to colonize microstructured scaffold lanes and thickness already at early time points (24 h) (Fig. 6 C).

To ascertain MSC and NMC adhesion and growth on the scaffolds, CellTiter-Blue assay was performed. A greater adhesion of both hMSCs and NMCs was measured on microstructured respect to non-microstructured scaffolds, while rMSCs adhered comparably on both scaffolds (Fig. 6 D). Proliferation analysis demonstrated that cells were able to proliferate only on microstructured scaffolds: after 15 days a significant proliferation was observed with a fold increase of 3.81 ± 0.5 (a.u.) (Fig. 6 E) for hMSCs and 5.21 ± 0.19 (a.u.) for NMCs (Fig. 6 E). rMSCs proliferated poorly on both scaffolds (Fig. 6 E).

Specific analysis of cell elongation (Fig. 6 F) confirmed that only on microstructured scaffolds both hMSCs and NMCs stretched out. hMSC showed an initial decrease in cell length by day 1, possibly due to space constraint (Fig. 6 F, d1, not significant vs. 2-D control culture), while NMCs immediately adopted a markedly elongated morphology (Fig. 6 F, d1, $p < 0.01$ vs. 2-D control culture). Both cell types reached the maximum elongation after 12 days of culture (Fig 6 F, d12, hMSCs: 145.54 ± 9.05 µm, $p < 0.0001$ vs. d1; NMCs: 136.59 ± 6.84 µm, not significant vs. d1). These results suggest that NMCs are more ready to assume an elongated shape.

During scaffold colonization cells maintained an optimal cytoskeletal organization (Fig 7 A) and they were able to colonize the entire construct thickness, growing in at least three cell layers as shown in the 3-D scaffold reconstruction (Figure 7 B) where the arrows indicate the different nuclei disposition.

Transmission electron microscopy analysis allowed to better analyze stem cell adhesion to the microstructured scaffolds. At lower magnification (Fig. 7 C, left panel) it is possible to observe that hMSCs adhered to the construct in different points (arrows) assuming an elongated shape and with long cytoplasmic processes. At higher magnification (Fig. 7 C, right panel) it is possible to better appreciate electron-dense areas, known as focal

adhesions or focal contacts, typically elongated, in which the plasma membrane runs parallel to the overlying matrix.

Taken together, our results demonstrate that MSCs and NMCs remained viable on both non-microstructured and microstructured scaffolds. In addition, on microstructured scaffolds, both cell types were forced to adopt a highly elongated and thin morphology and a distribution mimicking the 3-D cell alignment of myocardium. Therefore, we focused on the analysis of the possible cardio inductivity of microstructured PHBHV/gelatin scaffolds, which was obtained on the basis of decellularized suine myocardium.

3.3 Cardioinductivity of microstructured scaffolds

To evaluate whether the 15-day culture on the microstructured scaffolds influenced gene expression in both MSCs and NMCs with respect to 2-D control cultures, qPCR was performed for selected genes known to be involved in cardiomyogenesis and their expression was evaluated compared to 2-D control culture. In particular, transcript expression levels of stemness (Kit), early cardiac (Gata4, Mef2c) and late cardiac genes (Tbx5, Gja1, Tnnc1) were evaluated. The cardioinductivity experiments with mesenchymal stem cells were also performed with all four blends with comparable results; only representative images of some compositions will be shown. We observed that MSCs grown on microstructured scaffolds exhibited a reduced stemness expression (relative Kit expression level, -$\Delta\Delta$Ct, corresponding to -5.45 ± 0.29 for hMSCs and -2.19 ± 0.27 for rMSCs) together with an upregulation of early cardiac transcription factor Gata4 (-$\Delta\Delta$Ct 4.86 ± 0.7 for hMSCs and 2.56 ± 0.15 for rMSCs; Fig. 8 A), whose expression was undetectable in 2-D control culture. When transcript expression levels were evaluated on NMCs grown on the same scaffolds, Gata4 transcript, which was already expressed in 2-D control culture, was not further modulated; a decreased expression of Mef2c was observed (Fig. 8 B), although its residual expression was demonstrated by RT-PCR (Fig. 8 C); an

increased expression of late cardiac genes such as the transcription factor Tbx5 and the functional protein Gja1 were clearly detected and finally, upregulation of Tnnc1 was observed, though only on the 85/15 PHBHV/gelatin scaffold (Fig. 8 B).

Then, we evaluated if the increase in mRNA transcript levels was significant enough to drive to specific tissue lineage protein expression. As shown in figure 8 (D and E), hMSCs and rMSCs showed decreased expression of the stemness marker c-kit after 15-day culture on microstructured scaffolds and the early cardiac transcription factor GATA-4 was acquired, confirming qPCR results. NMCs acquired the expression of the early cardiac transcription factor Nkx2.5 as well as sarcomeric proteins like Troponin C and α-actinin and the structural protein Connexin 43 increased (Fig. 8 F), confirming previous gene expression data. However, the static culture on these scaffolds was not associated to striated organization of cardiac contractile proteins, thereby excluding the induction of a complete sarcomeric rearrangement in these cells.

Altogether, these results show the ability of our microstructured scaffolds to direct initial MSC and NMC lineage specification towards cardiomyogenesis in the absence of any external stimuli.

4. DISCUSSION

Here we demonstrate that the exploitation of the synergy between specific physico-chemical properties and the micropatterning of a bioartificial construct, mimicking structural and mechanical properties of the myocardium, and the differentiation potential of adult stem cells represents an opportunity to promote cardiomyogenesis in the absence of any external stimulus, avoiding nanofunctionalisation with cell-adhesive peptides or other biochemical signals. In fact stem cell adhesion and differentiation is strongly influenced by physico-chemical properties of the surface of biomaterials, including hydrophilicity, microporosity, that represent relevant signals for ECM-cells interactions. Since, chemical

nature, composition, molecular interactions of the material have an important role in the cellular response a deep understanding of the molecular interactions at nanoscale level represents a key point for the selection of scaffolds with suitable performances in regenerative medicine.

Chemical imaging technique is a useful and innovative tool to investigate about hydrophilicity and molecular interactions between material components. Maps acquired in µATR mode suggest that PHBHV/gelatin materials exhibit hydrophilicity properties matching those of healthy myocardium sample. In addition the study of scaffold surface was carried out by NIR spectroscopy highlighted the difference of hydrophilicity at level of ridges respect to recesses of the microstructure. In particular the interpretation of the NIR maps showed that the amount of OH groups respect to CH groups was higher in recesses than in ridges indicating a specific anisotropic surface hydrophilicity of the materials that can be fundamental to explain the behavior of stem cells seeded onto these matrices. FT-IR analysis showed the presence of interactions among functional groups of PHBHV and gelatin, particularly in the case of blends at lower gelatin content. These interactions could influence structural conformation of gelatin. In fact, the study of the secondary structure of the blend PHBHV/gelatin at various composition shown a shift from a quite disordered conformation to a more ordered structure and more similar to that of healthy natural tissue. This effect would suggest that the presence of non-fibrillar collagen-like sequences (type IV and VI) can favorably modulate stem cell behavior [41].

The evaluation of mechanical properties of PHBHV/gelatin systems showed that storage modulus resulted in the order of MPa, in both non and microstructured samples, being these values similar to the healthy cardiac tissue [42]. In addition, the anisotropic structure conferred by soft-lithography induced anisotropic mechanical properties with a higher storage modulus value in the longitudinal direction than that along the trasversal direction. We have also examined mechanical behavior of materials under water incubation, the

elastic modulus was found in both directions lower than that measured under dry conditions, indicating that mechanical properties of materials evaluated in physiological conditions exhibited values closer to native tissue.

Recently, the authors prepared and characterized 3-D microfabricated scaffolds by soft lithography reproducing cardiac ECM structure using different bioartificial materials [43, 44]. However these scaffolds have not proved effective in promoting adhesion and differentiation of stem cells in cardiac sense (unpublished results). The effects of these rectangular micropatterned bioartificial scaffolds were limited to their capacity to support proliferation and differentiation of model cells (C2C12 myoblasts) [43, 44]. In addition we must consider that the previously used bioartificial materials displayed different properties in terms of hydrophilicity, cristallinity and elastic modulus [43, 44]. For instance, using strain scan analysis, we registered higher storage modulus values of around 650-1200 MPa [43] and 68.4±1.0 MPa [44] for the different bioartificial systems tested.

Biodegradation properties of PHBHV/gelatin scaffolds was examined *in vitro* using different media and for prolonged times. Morphological analysis, pH trend of degradation solutions and GPC analysis confirmed a slow and gradual degradation of the scaffolds, the maintenance of a regular surface microstructure, an unaltered pH in the degradation media thus preventing possible inflammatory response *in vivo*. This biodegradation behavior is interesting because it allows to maintain unchanged the scaffold structure, thus playing a support role for cell growth and driving organization/differentiation of cells *in vitro* or *in vivo* for a long time.

While in most previous studies scaffolds have been credited with providing mere physical support for stem cell adhesion and proliferation, and geometrical guidance in tissue organization, whereas growth factors [4, 45, 46], physical stimuli [47, 48] or co-culturing with mature cardiomyocytes [49] have been considered as the major players in driving cell differentiation, our data show that the bioartificial construct per se substantially induced

cardiac commitment of MSCs and cardiac resident NMCs. There are growing evidence illustrating the potential to modulate stem cell differentiation via precise modulation of cell shape. In this setting, our construct provides, independently from the bioartificial blend composition, a means for extensive elongation of MSCs and cardiac resident NMCs on the structure, and allows cellular integration into a syncytium-like organization, both of which are important structural components to be considered to obtain a unified forceful contraction. Both MSCs and cardiac resident NMCs formed focal adhesions on PHBHV/gelatin substrate and microstructure recesses controlled their spatial distribution, favoring the cells to attach and grow within these regions and resulting in their dramatic elongation.

Recently the use of hydrogels based on fibrin and Matrigel [50] or PEG [51] in combination with specific cells has demonstrated functional differentiation characteristics of native myocardium. Alternative approaches concern with the use of scaffolds in solid state such as our construct that consents a rapid fabrication in a highly controlled and reproducible form. In addition the slow degradation kinetics of PHBHV/gelatin scaffold can ensure adequate stiffness for mechanical support *in vivo* at the site of lesion during the whole process of tissue regeneration. The scaffold designed in our study makes it possible the use of a patch to be inserted directly *in vivo* at early phase after myocardial infarction. With respect to the cell type, Liau et al. produced functional cardiac tissue patches from genetically purified mouse embryonic stem cell-derived cardiomyocytes and cardiovascular progenitors [50]. While this system offers unprecedented *in vitro* conditions capable of recapitulating important aspects of embryonic cardiac development, the need of embryonic stem cells limits its translation in clinical setting. Kim et al. combined rat cardiosphere-derived cells with nanotopographically defined hydrogels mimicking the native myocardial matrix and demonstrated induction of early cardiomyogenesis [51]. However, co-culturing with mature cardiomyocytes was needed to obtain expression of

mature cardiac markers such as punctuated patterned Cx43 and Troponin suggesting a lower cardioinductive potential compared to our construct. In our study both MSCs and NMCs displayed features of myocardial lineage after they were seeded on our 3-D scaffold only, without the need for any further stimuli. This may be advantageous *in vivo* heart where resident non myocytic precursor cells may migrate and differentiate within the exogenous applied 3-D scaffold. Both studies evidenced the pivotal role of cell elongation and alignment, which in the study of Liau et al. was necessary for the development of electrical properties[50] and in Kim et al., consistently with our study, for the expression of cardiac markers [51]. This cell distribution involves cytoskeletal re-organization that can therefore provide a physical stimulus by which mechanical deformation is translated into biochemical responses. In accordance, another recent study reported upregulation of cardiomyogenesis-associated genes in human bone marrow MSCs upon alignment and elongation on fibronectin printed lanes, in absence of soluble differentiation factors [52]. Intriguingly, Guan et al. observed that enhanced cardiac commitment was achieved by 3-D alignment of MSCs within an electrospinned polyurethane nanofiber construct [47]. While, however, in Guan's paper cultured MSCs maintained a round morphology and specific stretching of tissue constructs during culture was necessary to achieve cell alignment, we remark that cardiac ECM-like microstructure of our scaffold is able to drive optimal cell adhesion and alignment in the absence of external stimuli.

To our knowledge, only few studies addressed the influence of scaffold seeding on cardiac resident cells before. Forte et al. demonstrated the differentiation of cardiac progenitor cells into cardiomyocytes after culturing on different microfabricated scaffolds, yet by adding to the culture many cardiomyocyte-differentiating factors [53]. Finally, Gaetani et al. demonstrated that human cardiac progenitor cells could be printed in alginate scaffold and cultured *in vitro* to increase their cardiac commitment, even though, similarly to our results,

full cardiac differentiation was not achieved [54]. Thus, the use of resident NMCs for testing constructs for myocardial regeneration represents an innovative step ahead.

5. CONCLUSIONS

In this study we fabricated PHBHV/gelatin bioartificial constructs mimicking anisotropic structure and mechanical properties of the myocardium. These constructs, recapitulating a series of optimal properties in terms of hydrophilicity, chemical interactions, crystalline domains, protein structure, elastic modulus, anisotropic structure, showed their suitability in favoring stem cell adhesion and differentiation. The biodegradation behavior suggested the ability of these matrices to drive the growth and organization of cells for a prolonged time. This work represents a new approach to induce both non-resident and resident stem cells to cardiac commitment in a 3-D structure, without external stimuli. It is likely that MSCs and NMCs cultured on the scaffold together with an additional differentiation stimulus could reach a higher level of differentiation. However, this is beyond the scope of the present study, which aimed to show the possibility to obtain cardiac differentiation with the use of scaffold only. These tissue constructs have the potential to serve as patches for cardiac regeneration, without the need for cellularization with pre-induced cells, thus increasing the potentiality of organ repair. In addition, the developed bioartificial constructs may be used as an *ex vivo* microenvironment to investigate differentiation of different types of stem cells for cardiac therapy.

6. ACKNOWLEDGEMENTS

A

Microstructured scaffold surface   Microstructured scaffold section   Non-microstructured scaffold section

B

Longitudinal direction

Transverse direction

C

Dry

Wet

E (MPa)

Figure 1

Figure 2

Figure 3

A

95/05 PHBHV/gelatin   90/10 PHBHV/gelatin   80/20 PHBHV/gelatin

B

80/20 PHBHV/gelatin

90/10 PHBHV/gelatin

95/05 PHBHV/gelatin

Pure gelatin
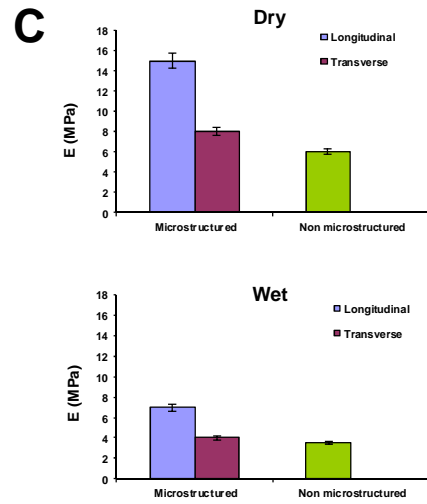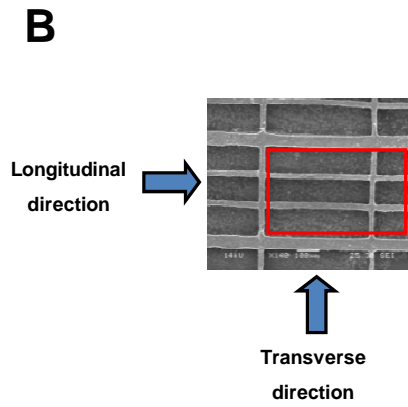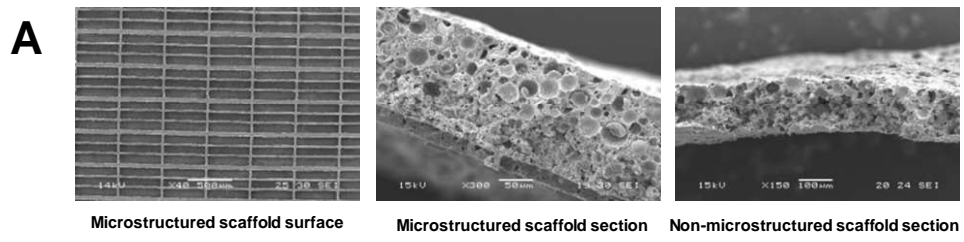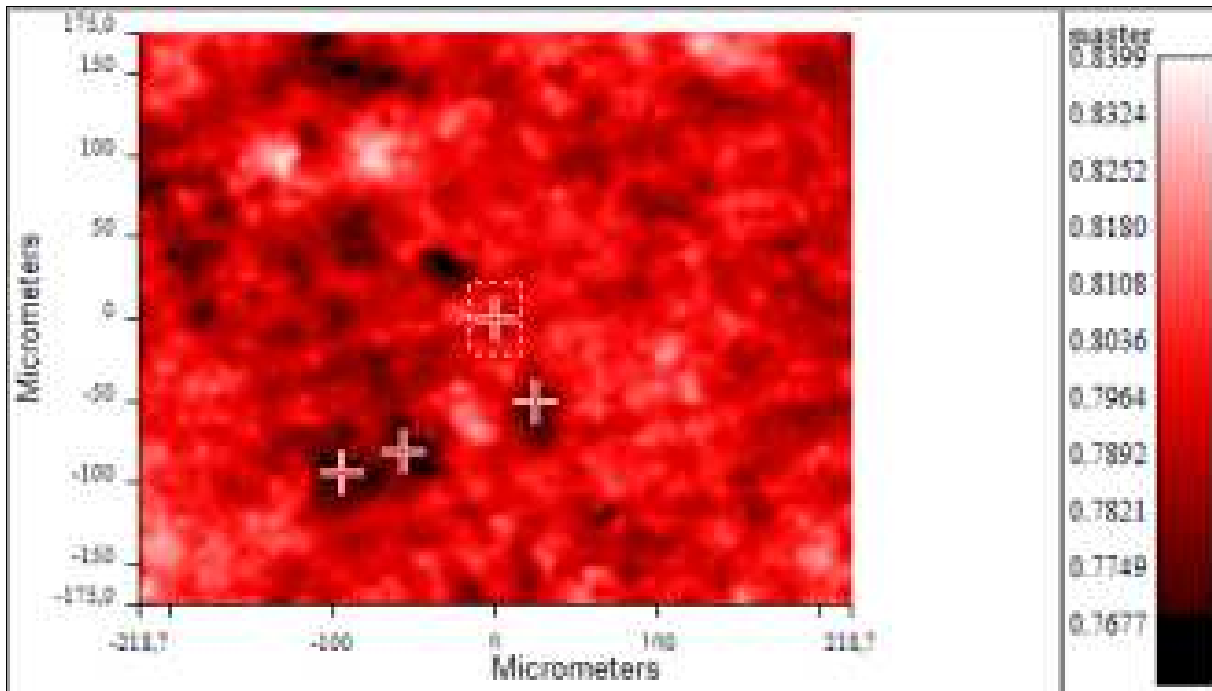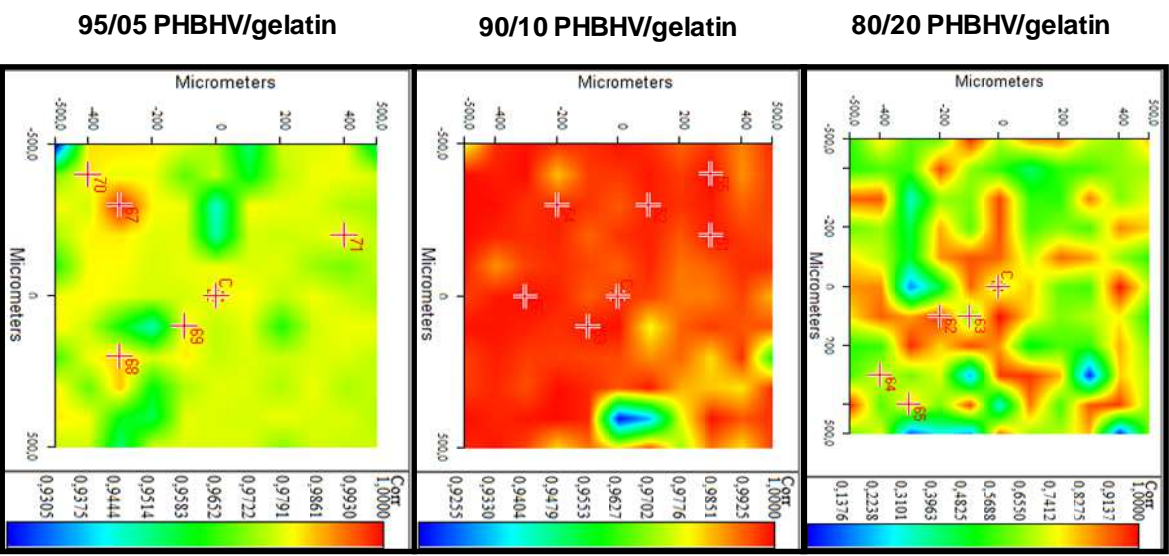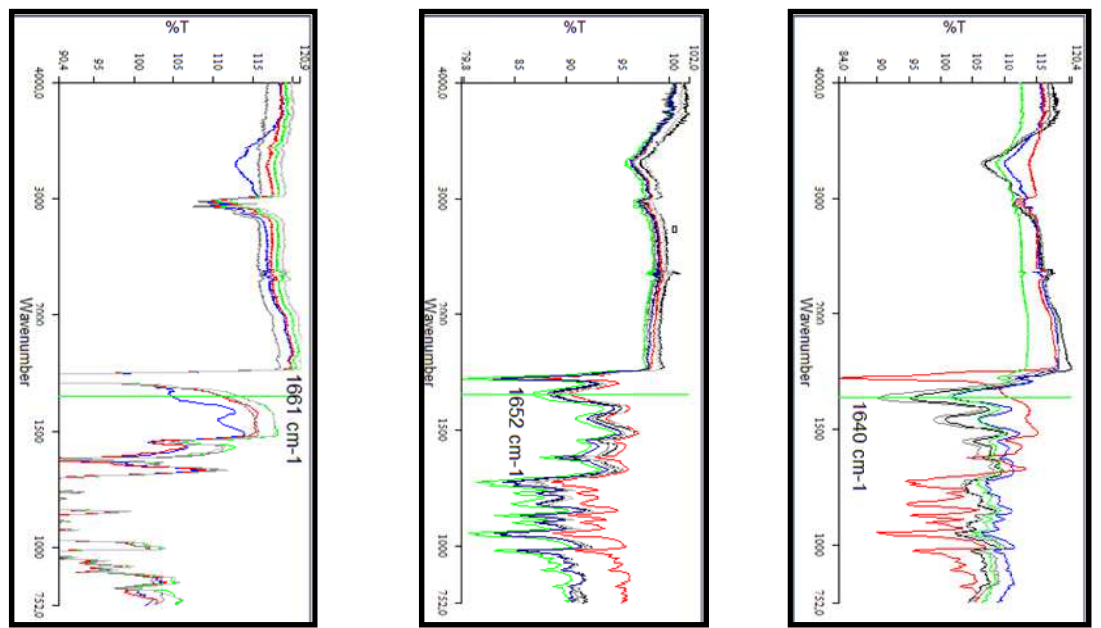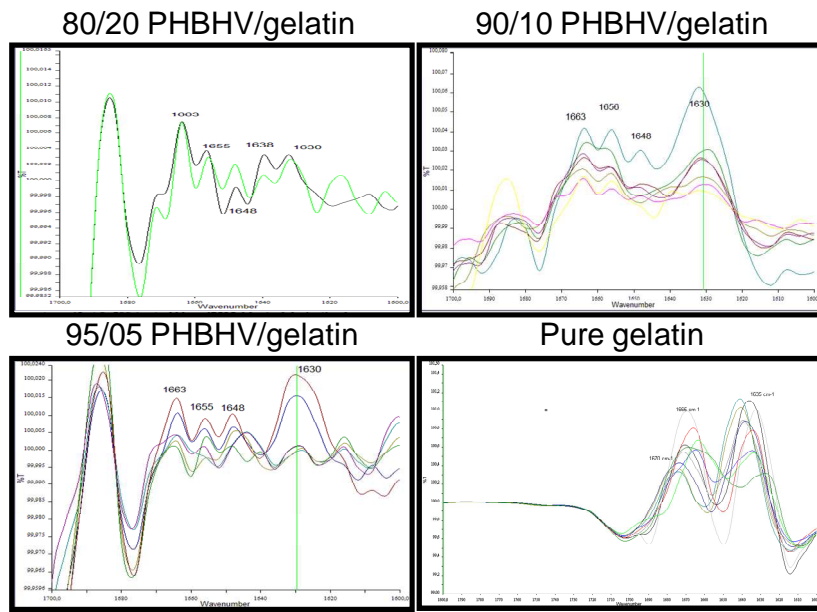
Figure 4

Figure 5

Figure 6

A Phalloidin/DAPI

B Phalloidin/DAPI

C

Figure 7

Figure 8